Int. J. Pure Appl. Sci. 9(2);411-421 (2023)

IJPAS
ijpas@munzur.edu.tr
ISSN: 2149-0910

Research article/Araştırma makalesi
DOI:10.29132/ijpas.1377054

Numerical Analysis of The Thin Film Solar Cell Modelled Based on In Doped CdS Semiconductor

Serap Yigit Gezgin[1], Silan Baturay[2], Hamdi Sukur Kilic[1,3,4,*]

[1]*University of Selcuk, Faculty of Science, Department of Physics, Konya, Türkiye*
[2]*Dicle University, Faculty of Science, Department of Physics, Diyarbakir, Türkiye*
[3]*University of Selcuk, Directorate of High Technology Research and Application Center, Konya, Türkiye*
[4]*University of Selcuk, Directorate of Laser Induced Proton Therapy Application and Research Center, Konya, Türkiye*
*serap.gezgin@selcuk.edu.tr, silan@dicle.edu.tr, *hamdisukurkilic@selcuk.edu.tr*
Received date:16.10.2023, Accepted date: 29.11.2023

Abstract

In this study, pure and 1%, 2% and %3 In-doped CdS thin films were produced by spray pyrolysis method. CdS is an *n*-type (II-VI group) semiconductor material and used as a buffer layer in solar cells. By doping In into CdS thin film, it was investigated how optical and crystalline behavior of thin film are changed. Using Moss and Herve&Vandamme and Ravindra relations, refractive indices and dielectric coefficients were investigated depending on the band gap of the obtained CdS sample. It has been observed that In element decreases the band gap of CdS thin film, improved its crystal structure and reduced its roughness. Therefore, 3% In doped CdS has gained a more ideal feature for use as an *n*-type semiconductor in solar cells. CIGS/In doped CdS solar cell was modelled and analysed by SCAPS-1D simulation program by using the physical parameters of the semiconductor layers that make up solar cells as imputs of program. Photovoltaic parameters of solar cell based on donor defect density, the neutral interface defect density and Auger electron/hole capture coefficient which were calculated by using In %3 doped CdS thin film, which has the most ideal *n*-type semiconductor properties.

Keywords: CdS, metal doping, simulation program, refractive indices

In Katkılı CdS Yarı İletkenine Dayalı Olarak Modellenen İnce Film Güneş Pilinin Sayısal Analizi

Öz

Bu çalışmada katkısız ve %1, %2 ve %3 In katkılı CdS ince filmleri sprey piroliz yöntemiyle üretildi. CdS, *n* tipi (II-VI grubu) bir yarı iletken malzemedir ve güneş pillerinde tampon katman olarak kullanılır. CdS ince filmine In katkılanarak, elde edilen ince filmin optik ve kristal özelliklerinin değişimi incelendi. Moss, Herve&Vandamme ve Ravindra bağıntıları kullanılarak elde edilen CdS filmlerinin bant aralığına bağlı olarak kırılma indisleri ve dielektrik katsayıları araştırıldı. In katkısı sonucu CdS ince filmin bant aralığı azaldı, kristal yapısı iyileştirildi ve pürüzlülüğü azaltıldı. Bu nedenle %3 In katkılı CdS, güneş pillerinde *n* tipi yarı iletken olarak kullanım için daha ideal bir özellik kazanmıştır. SCAPS-1D simülasyon programı kullanılarak CIGS/In katkılı CdS güneş pili, güneş pillerini oluşturan yarı iletken katmanların fiziksel parametreleri modellenmiştir. Güneş pilinin donör kusur yoğunluğu, nötr ara yüzey kusur yoğunluğu ve Auger elektron/hol yakalama katsayısına dayalı fotovoltaik parametreleri, en ideal *n*-tipi yarı iletken özelliklere sahip %3 In katkılı CdS ince filmi kullanılarak hesaplanmıştır.

Anahtar Kelimeler: CdS, metal katkı, simülasyon program, kırılma indisi

IJPAS
ijpas@munzur.edu.tr
ISSN: 2149-0910

Research article/Araştırma makalesi
DOI:10.29132/ijpas.1377054

INTRODUCTION

A variety of applications of thin film polycrystalline semiconductors in electronics and optoelectronics technologies have been attracted great interest as wel as explored over this industrial area. The optoelectronic property of cadmium sulphide (CdS) makes it very useful material for futured applications (Patida et. al., 2006). A polycrystalline device's low production cost is primarily responsible for its technological appeal. In solid state technology and fundamental research, thin films play an increasingly important role. CdS polycrystalline thin film is a representative semiconductor from the II-VI group of periodic tables of elements and it has been significantly studied as a window layer for application of thin film solar cells, due to its wide optical energy band gap of about 2.45 eV, a high electrical resistivity and high transmittance value.

CdS films have four different crystalline orientations. Three of these orientations, hexagonal rock salt, cubic distorted and cubic undistorted rock salt with zinc blended, are the most commonly met (Ziabari and Ghodsi, 2012). Among all these, the hexagonal crystalline structure is the most common and thermodynamically most stable of these changed crystalline orientations. It is possible to obtain a metastable phase of CdS with cubic structure (Rittner and Schulman, 1943). Additionally, it can be said that the cubic structure forms at room temperature. It is thought that CdS is a metastable phase, while hexagonal is a stable, and thermal annealing may often result in a phase formation from cubic to hexagonal structure (AlKhalifah et. al., 2020) The important fact for this formation of phase is understood to be around 300 °C (Zelaya-Angel et. al., 1994) Rock salt phase formation exists only in hydrostatic pressures ranging between 60 and 68 GPa (Ziabari and Ghodsi, 2012). Of these four different crystal orientations, it is evident that the undoped CdS sample exhibits the creation of distinct polymorphic phases (cubic and hexagonal). These phases are polycrystalline structure, and crystallinity of CdS films upsurges in response to varying annealing temperatures (Xu et. al., 2016). Xu et al. indicated that the main peaks in X-ray diffraction spectra of fabricated CdS film with In doping element can be indexed to the shape of hexagonal phase (Xu et. al., 2016). Kaur et al. (Kaur et. al., 1980) have proved that the homogenous samples with the production of cubic, hexagonal, or mixed of cubic and hexagonal phases are made of the results of the ion-by-ion method.

Fabrication procedures and related constraints have important impacts on nucleation and growing of samples and their crystallite and optical properties. Various physical and chemical methods including thermal evaporation (Sahay et. al., 2007), sol-gel spin coating (Seon et. al., 2009), the successive ionic layer adsorption and reaction (Sankapal et. al., 2000), MOCVD (Yoon et. al., 2006), electrostatic spray assisted vapor method (Su and Choy, 2000), and ultrasonic spray pyrolysis (Baykul and Balcioglu, 2000) have already been applied to produce such thin films. Ultrasonic spray pyrolysis relies on the thermal breakdown of the solution of source after it is sprayed on the thermally heated surface of substrate. Large-scale deposition of thin films can be achieved by adding elements to aqueous solutions (Bang et. al., 2007). Additionally, there is no need for a vacuum and no need for high-quality targets with this method. By regulating the spray settings, it is simple to manage the film deposition parameters and this technique is used in this work to grown undoped and In doped CdS samples on the soda lime glass because of its ease of use and adaptability. Computation of these applied photovoltaic (PV) parameters of solar cells can be performed by inputting specific physical factors of layers that comprise the solar cell into the SCAPS-1D algorithm. It is well noticed that the characteristics parameters of deposition and production process as well as layers produced, such as donor or acceptor defect densities, interface densities, operating temperatures, etc., have a great influence on the efficiency of layers in solar cells and can be used for performing calculations (Burgelman et. al., 2016; Tripathi et. al., 2020). Researchers can operate more safely and confidently thanks to the useful information these theoretical efficiency calculations for solar cells provide regarding the potential performance of solar cells to be created.

The effects of several factors such as annealing time, thickness of thin film, and metal doping ratio have been examined so far. These deposition parameters have improved the physical properties including crystallite parameters, and optical behavior of obtained films, and this has led the researchers to improve the physical properties of CdS films to be obtained by using doping metals. While the physical

IJPAS
ijpas@munzur.edu.tr
ISSN: 2149-0910

Research article/Araştırma makalesi
DOI:10.29132/ijpas.1377054

characterization of CdS film have been studied by groups (Ashour, 2003; Petrus et. al., 2020; Sahay et al., 2007). SCAPS 1-D calculations of undoped and In:CuO films using USP method to confirm and to calculate the effect of various features on solar cells have not comprehensively been studied. Therefore, both theoretical and experimental calculations are essential to better identify the impact of In-doping on the physical behavior of the undoped CdS film.

MATERIAL AND METHODS

The first of all, the undoped and In doped CdS films have been deposited on SLG substrate using USP method. Before fabrication, SLG as a substrate was washed to ensure high-quality CdS samples on cleaned surface. Five stages were used for substrate cleaning process: For the first step, substrates were boiled for 20 minutes at 120 degrees Celsius in a solution of deionized water (H_2O), ammonia (NH_3), and hydrogen peroxide (H_2O_2), followed by 20 minutes at 120 degrees Celsius in a solution of H_2O, H_2O_2, and hydrochloric acid (HCL). Then, it was ultrasonicated in acetone and distilled water for 3 min, respectively.

After the cleaning process, these substrates dried in N_2 gas. A stoichiometric amount of 0.01M Cd ($C_4H_6CdO_4$) and 0.01 M thiourea (CH_4N_2S) as sources of cadmium and sulphur ions in distilled water were used to prepare homogenous CdS films due to the environmentally friendly solvent. Indium chloride ($InCl_3$) was used for In doping with concentration (1, 2, and 3 at % In). Using an ultrasonic nebulizer with a 125 kHz frequency, the prepared solution was atomized onto SLG. The obtained homogenous solution was sprayed using this technique onto substrate heated at around 275 °C at for 30 minutes constantly immovable nozzle–substrate separation of around 9.5 cm. The nozzle of USP was worked at 125 kHz during spraying process. 50 cc of obtained homogenous solution was sprayed onto cleaned SLG about 50 min. Flow metering was used to maintain a 1 mL/min flow rate of solution with N_2 gas being transported to the substrate to avoid oxide formation. The mechanized nozzle of USP was continuously shifted in the x-y directions at 15 mm/s to give homogeneous insurance. Undoped and In:CdS samples were annealed at 500 °C in N_2 to investigate the In doping impact on solar cells parameters.

The structural properties of the obtained film on SLG were achieved using X ray diffractometer (XRD) with Cu kα radiation (λ=1.542 Å). The change in band gap change and absorbance of the obtained samples to investigate the optical properties of samples was determined in UV-Vis spectrophotometer measurement system in the wavelength range of 300–1100 nm. In addition, CdS thin film based solar cell is modelled by SCAPS-1D software. The effects of various contacts i.e. Ni, Ag, Cu, Mo, and Au on the formed solar cells' efficiency have been studied.

RESULTS AND DISCUSSION

Structural Properties

Fig. 1 (a) displays XRD patterns of undoped and In:CdS films compound of II-VI group formed by USP at different doping ratio. The XRD pattern of undoped and In:CdS samples annealed in N_2 ambient at 500 °C reveal polycrystalline nature. Undoped CdS film, annealed at 500 °C, indicates the presence of three peaks around 25.68°, 26.77° and 44.00° corresponding to (100), (002) and (110) planes of both hexagonal and cubic structures. Three main peaks in XRD spectrum for In:CdS clearly demonstrate the polycrystalline character of the material, and their diffraction angles are approximately 25.50°, 26.66°, and 44.00° corresponding to (100), (002), and (110) planes of hexagonal structures, respectively. In all films, the peak about 26.66° shows the most preferred orientation along the (002) plane of structure of hexagonal, indicating its better crystalline nature and suitability for photocatalysis (Gao et al., 2019). Perna et al. (Perna et al., 2004). have indicated that XRD spectra consist of a peak placed at around 26.5° corresponding to the preferred orientation of the pure CdS lattice rising in a hexagonal structure. The intensity of the preferred orientation improved with increasing In concentration and the intensity of all CdS peaks increased as the In concentration ratio of thin films increased and In:CdS peak becomes narrower compared to undoped CdS film. In general, one can conclude that the introduction of In into CdS promotes the crystallization process. Atay et al. (Atay et. al., 2003) have indicated that the angular width value of the peak at the full width at half maximum (FWHM) are increasing and crystallite size (D) are decreasing with In doping when compared with undoped CdS sample because of the fact that crystallinity is worsen and a reduction in the (002)

IJPAS
ijpas@munzur.edu.tr
ISSN: 2149-0910

Research article/Araştırma makalesi
DOI:10.29132/ijpas.1377054

plane with a decreased crystallite size value was noted with the In ratio.

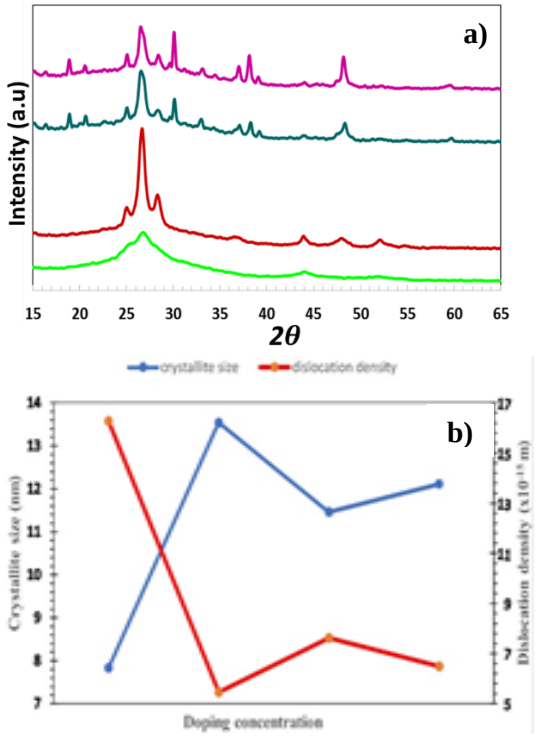

Fig. 1a) XRD pattern and **b)** Behavior of the In:CdS films' crystallite size and dislocation density

The crystallite size (D) is calculated related to β value using the Debye–Scherrer Formula.

$$D = \frac{0.94\lambda}{\beta \cos\theta} \quad (1)$$

where λ is the wavelength of X-Ray output of diffractometer, with Cu kα radiation (λ=1.542 Å), θ is the Bragg diffraction angle, β is the FWHM value in radian. The calculated D values of these films are given in previous study and depicted in Fig. 1(b); The calculated grain sizes of (002) growth of CdS film were radically increased as increasing In doping ratio in CdS. It can be said that the crystallite size of undoped CdS film changed with In doping. As In doping rati increases from 0% to 3%, the diffraction peaks of CdS films become sharper due to the fact that the crystals inosculate more easily and subsequently resulting in larger crystals. The dislocation density value (δ) of these films, which point to the density of defects in the lattice, was determined related to D value via the following calculation:

$$\delta = \frac{1}{D^2} \quad (2)$$

The micro-strain (ε) of the films was calculated as follows:

$$\varepsilon_{str} = \frac{\beta}{4\tan\theta} \quad (3)$$

The dislocation density in the film changed related to In doping ratio and seen in table 1. The lowest dislocation density value and highest D value has gained for 3% In:CdS film at 500 °C. Some decrease in the dislocation density of the obtained sample related to In doping gives fixed crystalline structure. The imperfections number in CdS films clearly decreases as In doping increases in Cd solution. Table 1 displays that as D value increases, micro-strain in the obtained samples decreases and this gives a high-quality crystalline films, which was calculated in previous study (Baturay, 2017). In fact, the large number of In atoms does not significantly damage CdS lattice; this confirms its good structural quality. It can be said that micro-strain plays an important role in determination of the physical properties of obtained thin. This increase in the crystallite size may have caused lattice micro-strain that resulted in the decrease observed in the energy band of doped films grown at 500 °C N_2 ambient.

IJPAS
ijpas@munzur.edu.tr
ISSN: 2149-0910

Research article/Araştırma makalesi
DOI:10.29132/ijpas.1377054

Table1. *Crystallite values of the In:CdS films*

Sample	2θ	FWHM	D (Å)	ε
Pure CdS	25.68	3.219	26.5	0.78
	26.77	1.091	82.0	0.27
	44.00	0.984	86.7	0.23
1% In:CdS	25.07	0.38	237.8	0.09
	26.66	0.65	140.0	0.16
	43.93	0.51	187.6	0.12
2% In:CdS	25.07	0.28	117.4	0.07
	26.63	0.77	167.3	0.19
	43.96	0.54	166.3	0.13
3% In:CdS	25.07	0.25	367.1	0.06
	26.61	0.67	134.8	0.16
	44.00	0.18	489.5	0.04

The optical properties of the In:CdS thin film

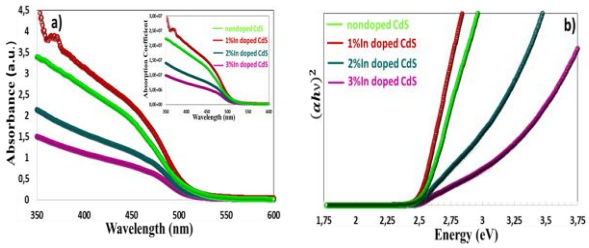

Fig. 2a) The absorbance and **b)** Tauch Plots of In:CdS film

The optical behaviors of the obtained CdS films were comprehensively analyzed to determine the effect of In doping on the energy band gap (E_g) and the absorbance value at room temperature. UV-Vis spectroscopy was used for calculation of these measurements over the wavelength range of 300–1100 nm. In UV-Vis region weren't seen any other peaks. Therefore, it is said that the obtained CdS thin films were uncontaminated, uniform, and of high-quality crystal structure. According to Fig. 3, all of these films show a strong absorption drop at the central absorption band edge as well as weak absorption value, which is related to electron excitation from the valence band (VB) to the conduction band (CB).

It is the difference in In dopant that causes the observed changes in optical absorption. Another words, it can be understood that the absorbance value of non-doped CdS sample is changed due to the different crystallinity and the roughness (Baturay, 2017). The optical behavior of CdS sample with different In doping were evaluated to investigate the effect of doping ratio on the E_g. UV-Vis spectroscopic measurement system was used for this measurement. Figure 2b shows the optical E_g value of CdS thin samples at room temperature. For such semiconductor materials, optical absorption theory displays the absorption coefficient (α) of the film and incident photon energy ($h\nu$) behaves as follows:

$$\alpha h\nu = A(h\nu - E_g)^n \quad (4)$$

where A is an energy-independent constant related to the material. A graph of $\alpha h\nu^2$ vs. photon energy ($h\nu$) for CdS samples as given in Fig. 2b indicates the effect of In doping on the energy band gap. The calculated E_g value of CdS with In doping from this graph is changed from 2.53 to 2.47 eV, which point to that In doping could be used to adjust the optical E_g value of CdS samples. The following equation (Eq. (5)) is used to calculate the absorption coefficient (α) of the obtained samples (Mustafa, 2013):

$$\alpha = 2.303(A/T) \quad (5)$$

A is absorption and T is thin film thickness. Similar to the absorption spectrum, 1% In doped CdS thin film has shown the highest absorption coefficient, while 3% In doped CdS thin film has presented the lowest. All non-doped and In doped CdS thin films have exhibited some higher absorption coefficients in UV region, as do n-type semiconductors. Accordingly, 2% and 3% In doped CdS thin films offer more ideal optical properties for use as transparent *n*-type semiconductors in thin film solar cells.

In second generation solar cells, *n*-type semiconductors must be highly transparent and have low refractive index (n) in order to transmit light directly to *p*-type absorber semiconductor without more absorption. The refractive index of the non-doped and In doped CdS thin films can be calculated

IJPAS
ijpas@munzur.edu.tr
ISSN: 2149-0910

Research article/Araştırma makalesi
DOI:10.29132/ijpas.1377054

by Moss relation expressed in Eq. (6) (Gezgin and Kiliç, 2022) and have been given in Table 2.

$$E_g n^4 = k \quad (6)$$

where, k, is a constant indicated to 108 eV. According to the values obtained from Moss relation, thin films have low refractive index, and especially the refractive indices of 2% and 3% In doped CdS thin films are even lower than others. The fact that these thin films have a lower absorption coefficient causes their refractive index to be lower.

Table 2. *Refractive index, high frequency dielectric constant and static dielectric constant of the non-doped and In:CdS thin films*

Samples	E_g (eV)	Moss relation		Herve&Vandemme		Ravindra		Static Dielectric Constant, ε_o
		n	ε_∞	n	ε_∞	n	ε_∞	
Nondoped CdS	2.53	2.55	6.53	2.50	6.26	2.01	4.04	10.73
1%Indoped CdS	2.50	2.56	6.57	2.51	6.31	2.03	4.14	10.82
2%Indoped CdS	2.47	2.57	6.61	2.52	6.37	2.06	4.24	10.91
3%Indoped CdS	2.47	2.57	6.61	2.52	6.37	2.06	4.24	10.91

Herve&Vandamme have revealed the relationship between n and E_g using Eq. (7) (Gezgin, 2022).

$$n = \sqrt{1 + \left(\frac{A}{E_g + B}\right)^2} \quad (7)$$

A and B are numerical constants having values of 13.6 eV and 3.4 eV, respectively. According to Table 2, the refractive indices obtained using Moss and Herve&Vandamme relations are very close to each other. Thence, the accuracy of both relations has been ensured. The refractive index increases with decreasing band gap.

Ravindra has used n and E_g in the different relation shown in Eq. (8) and expressed the relationship between them (Ravindra et. al., 2007):

$$n = 4.16 - 0.85E_g \quad (8)$$

As seen in the Table 2, Ravindra's relation has given results in a slightly lower value of refractive index compared to other relations. This is due to the numerical relationship used in Ravindra relation being slightly less adequate.

The electrical field formed by photo-excited charge carriers formed in the side of the depletion region of solar cell is determined by the dielectric constant of thin films. The high frequency-dielectric constant (ε_∞) and the static-dielectric constant (ε_o) which were expressed by Eq. (9) and Eq. (10), respectively:

$$\varepsilon_\infty = n^2 \quad (9)$$

$$\varepsilon_o = 18.52 - 3.08E_g \quad (10)$$

The high dielectric coefficient prevents the recombination of charges within the semiconductor and allows charges to reach the boundary of the depletion region without undergoing recombination within traps and defects. As seen in Table-2, 2% and 3% In doped CdS thin films indicated higher dielectric constants. The fact that the crystal structures of these thin films are more developed indicates that they have more defects and traps and that the life time of the charge carriers can be longer. This is consistent with their high dielectric constant.

The modelling of Au/CIGS/In doped CdS/i-ZnO/AZO solar cell

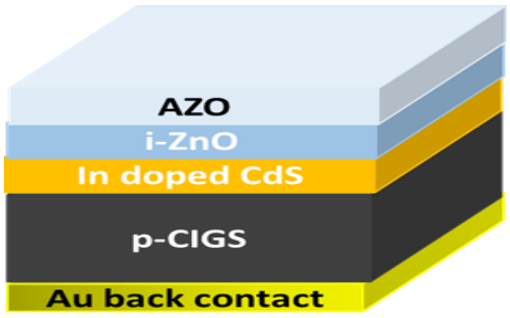

Fig.3. The schematic image of Au/CIGS/In doped CdS/i-ZnO/AZO solar cell modeled with the SCAPS

Possible performances of thin film solar cells consisting of different semiconductor layers can be determined with SCAPS-1D program. PV parameters can be calculated by entering the physical parameters of the layers such as band gap, electron affinity, electron/hole mobility, the shallow donor/acceptor density, etc. into the simulation program (Burgelman et. al., 2016; Tripathi et. al., 2020). 3% In-doped CdS

IJPAS
ijpas@munzur.edu.tr
ISSN: 2149-0910

Research article/Araştırma makalesi
DOI:10.29132/ijpas.1377054

thin film with 2.47 eV band gap is the most ideal semiconductor to be used as a buffer layer in solar cells, with its larger grain size and advanced crystal structure. In this study, the band gap, film thickness, dielectric coefficient and absorption coefficient files of the experimentally produced 3% In doped CdS thin film were entered into the simulation program as imput and Au (back contact)/CIGS (absorber)/In doped CdS (buffer) /i-ZnO (window) /AZO (front electrode) solar cell was modelled. PV parameters of the modeled solar cell were calculated depending on the interface neutral defect density, shallow donor defect density, and Auger electron/hole capture coefficient. The physical parameters of the layers forming the modelled In doped CdS/CIGS solar cell are presented in Table 3.

Table. 3. *The physical parameters of the layers forming the modeled In:CdS/CIGS solar cell*

Layers	AZO	i-ZnO	3% In doped CdS	CIGS
Band Gap (eV)	3.3	3.3	2.47	1.15
Electron affinity (eV)	4.6	4.6	4.2	4.6
Dielectric permittivity (relative)	9	9	10.91	13.6
CB effective density of states (cm^{-3})	$2.20x10^{18}$	$2.20x10^{18}$	$2.20x10^{18}$	$2.20x10^{18}$
VB effective density of states (cm^{-3})	$1.80x10^{19}$	$1.80x10^{19}$	$1.80x10^{19}$	$1.80x10^{29}$
Electron/Hole thermal velocity (cm/s)	$1.00x10^{7}$	$1.00x10^{7}$	$1.00x10^{7}$	$1.00x10^{7}$
Electron/Hole mobility (cm^2/Vs)	100/25	100/25	100/25	100/25
Shallow donor density (cm^{-3})	$1.00x10^{20}$	$1.00x10^{5}$	0	0
Shallow acceptor density (cm^{-3})	0	0	$1.00x10^{18}$	$6.5x10^{16}$
Thickness (nm)	100	50	350	2000

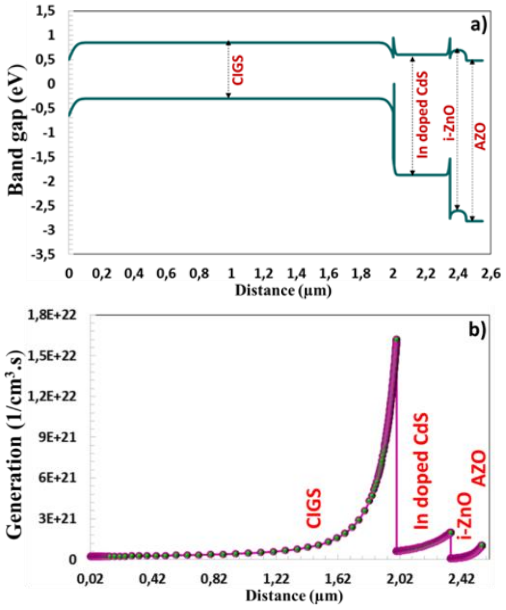

Fig. 4. a) The band gap and **b)** generation vs distance of CIGS, In:CdS, i-ZnO and AZO

According to the band diagram of solar cell shown in Fig. 4a, spike like conduction band is formed between CIGS and In:CdS semiconductors. The spike like conduction band results in favorable charge transition in the depletion region and prevents the recombination of electron and hole charge carriers in traps and defects near the interface (Gao et. al., 2019; Gansukh et. al., 2020; Ghorbani, 2020). The spectrum in Fig. 4b shows the distance-dependent charge formation in semiconductors. Accordingly, maximum charge generation occurs inside CIGS semiconductor (close to the depletion region). While the charge in 6.05×10^{20} ($1/cm^3s$) formed at the border (2,0001 µm) of the depletion region of In doped CdS, the charge in (2×10^{21} ($1/cm^3s$) occurred in the contact region (2,35µm) with i-ZnO semiconductor. Since the light comes from the upper region, highly photo-excited charge carriers are formed at the first entrance through In doped CdS the thin film. However, when the In doped CdS thin film is highly transparent, less charge generation occurs at the deflection limit because light is transmitted in higher amounts (Abderrezek and Djeghlal, 2019; Niane et. al., 2018).

Int. J. Pure Appl. Sci. 9(2);411-421 (2023)

IJPAS
ijpas@munzur.edu.tr
ISSN: 2149-0910

Research article/Araştırma makalesi
DOI:10.29132/ijpas.1377054

The photovoltaic properties of CIGS/In doped CdS solar cell based the shallow donor density (N_d) of In doped CdS thin film

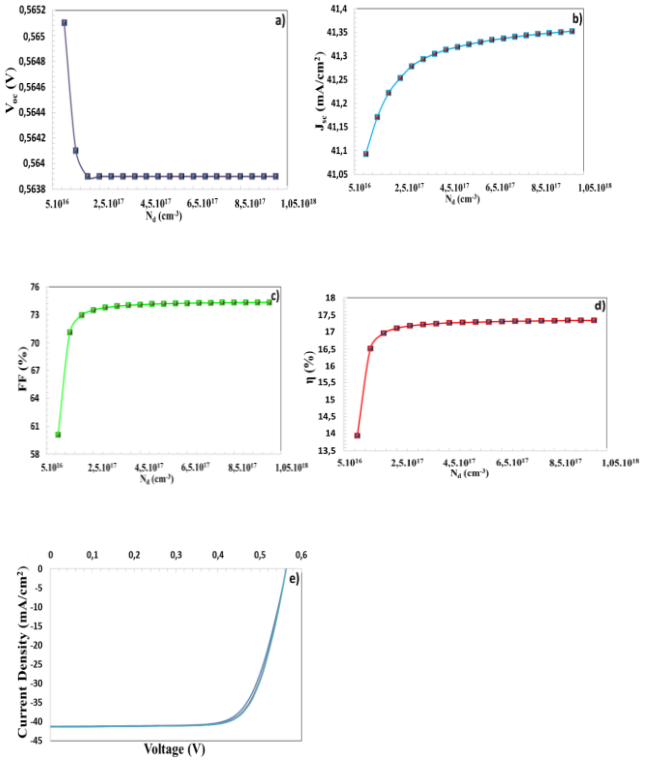

Fig. 5. (a-d) V_{OC}, J_{SC}, FF, η parameters **e)** $J-V$ characteristics CIGS/In:CdS solar cell vs N_d

The shallow donor defects are a factor that determines the *n*-type electrical property of the semiconductor. Increasing the shallow donor defect density (N_d) increases the *n*-type electrical conductivity of thin film and can improve the performance of the solar cell (Candan et. al., 2022). According to graphs repsented in Fig. 5a, when N_d was increased from 10^{-17} cm^{-3} to 10^{-18} cm^{-3}, V_{OC} value of solar cell first decreased from 0.565 mV to 0.563 mV and then stabilized. The J_{SC} value showed a parabolic rise, increasing from 41.0936 mA/cm^2 to 41.3522 mA/cm^2. When N_d value increased from 1×10^{-17} cm^{-3} to 1.5×10^{-17} cm^{-3}, FF and η values enhanced significantly and then increased slightly (N_d=1.5×10^{-17} cm^{-3} to 1×10^{-18} cm^{-3}). This case shows that no significant change was observed in PV parameters of solar cell after N_d= 1.5×10^{-17} cm^{-3}. According to literature, N_d = 1.10^{-18} cm^{-3} is accepted for *n*-type semiconductor and if this situation is taken as a reference, PV parameters of CIGS/In doped CdS solar cell are V_{OC}=0.563 mV, J_{SC}=41.3522 mA/cm^2, FF=74.33%, η=17.33%. In $J-V$ characteristics in Fig. 5e, there was a slight change in the curve with some rise of N_d.

The photovoltaic properties of CIGS/In:CdS solar cell based the neutral interface defect density

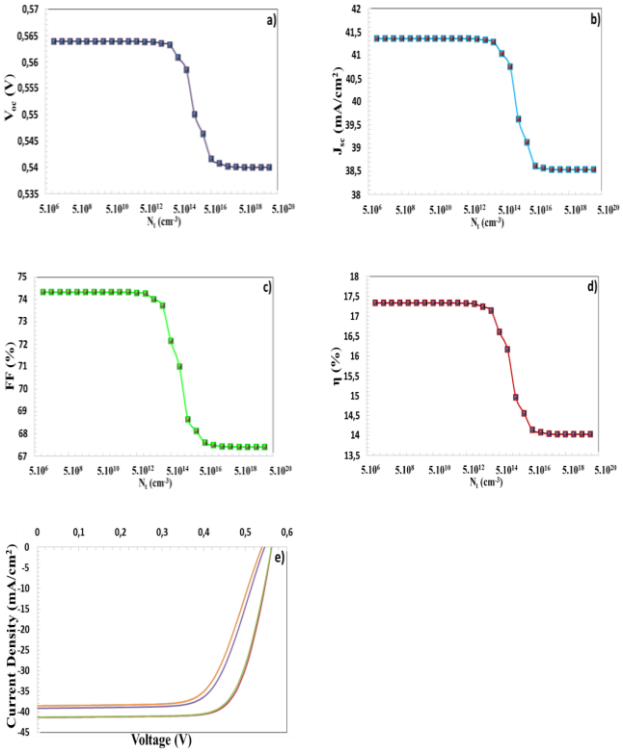

Fig. 6. (a-d) V_{OC}, J_{SC}, FF, η parameters and **e)** $J-V$ characteristics CIGS/In:CdS solar cell vs N_t

In heterojunction solar cells, defects at the interface in the depletion region cause the recombination of electron and hole charge carriers (Candan et. al., 2023). Properties, mismatch band alignment between *p* and *n*-type semiconductors, film resistance of these semiconductors, pinhole formations in the semiconductor and their surface roughness, number of grain boundaries in the film may cause the defects at the interface. These defects, which act as recombination points, cause deterioration in the performance of solar cell (Pindolia et. al., 2022; Srivastava et. al., 1990). For neutral interface defect density; N_t=1×10^{7} cm^{-3} and 1×10^{13} cm^{-3} and N_t=1×10^{21} cm^{-3} and 1×10^{27} cm^{-3}. The parameters of solar cell, are almost constant and the operating performance is not affected. However, as $N_t$is increased from 1×10^{13} cm^{-3} to 1×10^{21} cm^{-3}, solar cell efficiency drops significantly. This change can also be observed in $J-V$ shown in Fig. 6e.

IJPAS
ijpas@munzur.edu.tr
ISSN: 2149-0910

Research article/Araştırma makalesi
DOI:10.29132/ijpas.1377054

Therefore, in order to prevent decrease in the efficiency of solar cell, N_t value should not exceed $1x10^{13}$ cm^{-3}.

The Auger electron/hole capture coefficient on the photovoltaic properties of CIGS/In:CdS solar cell

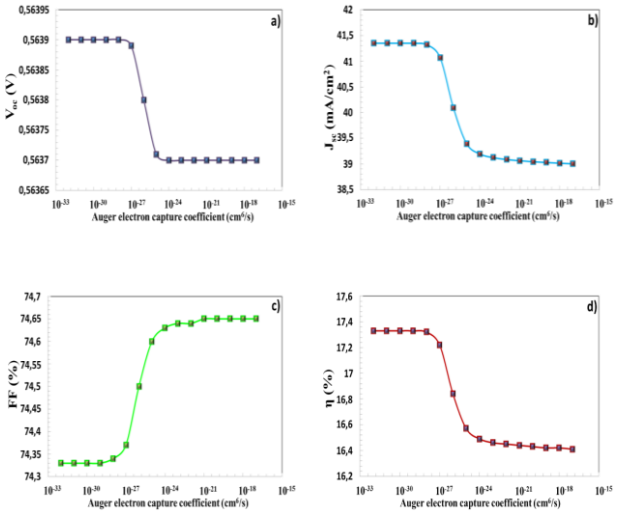

Fig. 7. (a-d) V_{OC}, J_{SC}, FF and η parameters vs Auger electron capture coefficient

Auger capture refers to a non-radiative recombination event (Hausser et. al., 1990; Strauss et. al., 1993). That is, high amounts of energy are released by the recombination of electron and hole charges. Electrons and holes in the same band are excited by this energy and transition to a higher energy level. This event is called as Auger electron/hole capture. While there was no change in the values of PV parameters until Auger electron capture coefficient was 10^{-28} cm^6/s, there was a noteworthy decrease in V_{OC}, J_{SC}, and FF values after 10^{-27} cm^6/s. Auger electron capture coefficient of In-doped CdS semiconductor, which has an electron majority charge carrier, is quite low and should not exceed 10^{-27} cm^6/s to avoid a decrease in efficiency of the solar cell.

In-doped CdS thin film, which has a hole minority charge carrier, has a higher Auger hole capture coefficient as seen in Fig. 8. There was a significant decrease in V_{OC}, J_{SC}, and η parameters between 10^{-20} cm^6/s and 10^{-16} cm^6/s. Therefore, as long as Auger hole capture coefficient does not exceed 10^{-20} cm^6/s, there will be no decrease in the efficiency of the solar cell.

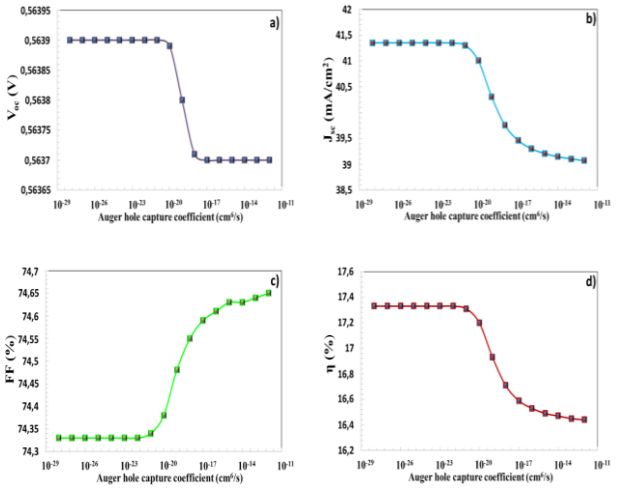

Fig. 8. (a-d) V_{OC}, J_{SC}, FF, η parameters vs Auger hole capture coefficient

CONCLUSION

The pure and 1%, 2% and 3% In doped CdS thin film was produced by spray pyrolysis method. The doped In element increased the grain size of CdS thin film reduces the band gap and improved its crystal structure. Using Moss and Herve&Vandamme and Ravindra relations, the refractive indices and dielectric coefficients of semiconductors were calculated. With decreasing band gap, the refractive index and dielectric coefficients increases. 3% In-doped CdS thin film in 2.47 eV band gap that is the most ideal semiconductor to be used as a buffer layer in solar cells, with its larger grain size and advanced crystal structure. Mo/CIGS/In doped CdS/i-ZnO/AZO solar cell was modeled with the SCAPS-1D program using an experimentally obtained physical parameters of 3% In doped CdS semiconductor. PV parameters of this solar cell were calculated depending on the neutral interface defect density, the donor defect density and Auger electron/hole capture coefficient. As a result, PV parameters of the optimized solar cell were determined as V_{OC}=0.563 mV, J_{SC}=41.3522, FF=74.33% and η=17.33%.

ACKNOWLEDGMENT

Authors would kindly like to thank to Selcuk University, Scientific Research Projects (BAP) Coordination Office for the support with the number 15201070 and 19401140 projects

IJPAS
ijpas@munzur.edu.tr
ISSN: 2149-0910

Research article/Araştırma makalesi
DOI:10.29132/ijpas.1377054

Selçuk University, High Technology Research and Application Center (İL-TEK) and SULTAN Center for infrastructures

Dr. Marc Burgelman's group, University of Gent, Belgium for providing permission for us to use SCAPS-1D simulation program.

CONFLICT OF INTEREST

The Authors report no conflict of interest relevant to this article.

RESEARCH AND PUBLICATION ETHICS STATEMENT

The authors declare that this study complies with research and publication ethics.

REFERENCES

Abderrezek, M. and Djeghlal, M. E. (2019). Contribution to improve the performances of Cu_2ZnSnS_4 thin-film solar cell via a back surface field layer. Optik, 181, 220-230.

Al-Douri, Y., Khasawneh, Q., Kiwan, S., Hashim, U., Abd Hamid, S. B., Reshak, A. H., Bouhemadou, A., Ameri, M. and Khenata, R. (2014). Structural and optical insights to enhance solar cell performance of CdS nanostructures. Energy Conversion and Management, 82, 238-243.

AlKhalifah, M. S., El Radaf, I. M. and El-Bana, M. S. (2020). New window layer of $Cu_2CdSn_3S_8$ for thin film solar cells. Journal of Alloys and Compounds, 813, 152169.

Ashour, A. (2003). Physical properties of spray pyrolysed CdS thin films. Turkish Journal of Physics, 27(6), 551-558.

Atay, F., Bilgin, V., Akyuz, I. and Kose, S. (2003). The effect of In doping on some physical properties of CdS films. Materials Science in Semiconductor Processing, 6(4), 197-203.

Bang, J. H., Han, K., Skrabalak, S. E., Kim, H. and Suslick, K. S. (2007). Porous carbon supports prepared by ultrasonic spray pyrolysis for direct methanol fuel cell electrodes. The Journal of Physical Chemistry C, 111(29), 10959-10964.

Baturay, Ş. (2017). Indium doping on the structural, surface and optical properties of CdS thin films prepared by ultrasonic spray pyrolysis method. Balıkesir Üniversitesi Fen Bilimleri Enstitüsü Dergisi, 19(2), 264-274.

Baykul, M. C. and Balcioglu, A. (2000). AFM and SEM studies of CdS thin films produced by an ultrasonic spray pyrolysis method. Microelectronic Engineering, 51, 703-713.

Burgelman, M., Decock, K., Niemegeers, A., Verschraegen, J. and Degrave, S. (2016). SCAPS manual. University of Ghent: Ghent, Belgium.

Candan, I., Gezgin, S. Y., Baturay, S. and Kılıç, H.S. (2023). Production of Cu_2SnS_3 thin films depending on the sulphur flow rate and annealing temperature time. Journal Of Optoelectronıcs and Advanced Materıals, 25(3-4), 191-202.

Candan, I., Gezgin, S. Y., Baturay, S. and Kilic, H. S. (2022). Structural, Morphological, Optical Properties and Modelling of Ag Doped CuO/ZnO/AZO Solar Cell. Journal of Coating Science and Technology, 9, 26-37.

Gansukh, M., Li, Z., Rodriguez, M. E., Engberg, S., Martinho, F. M. A., Mariño, S. L., Stamate, E., Schou, J., Hansen, O. and Canulescu, S. (2020). Energy band alignment at the heterointerface between CdS and Ag-alloyed CZTS. Scientific Reports, 10(1), 18388.

Gao, H., Wang, F., Wang, S., Wang, X., Yi, Z. and Yang, H. (2019). Photocatalytic activity tuning in a novel Ag_2S/CQDs/$CuBi_2O_4$ composite: Synthesis and photocatalytic mechanism. Materials Research Bulletin, 115, 140-149.

Gezgin, S. Y. (2022). Modelling and investigation of the electrical properties of CIGS/*n*-Si heterojunction solar cells. Optical Materials, 131, 112738.

Gezgin, S. Y. and Kiliç, H. Ş. (2022). The Effect of Ag and Au Contacts on the Efficiency of CZTS/*n*-Si Solar Cell: The Confirmation of Experimental and Theoretical Results by SCAPS Simulation. Brazilian Journal of Physics, 52(4), 148.

Ghorbani, E. (2020). On efficiency of earth-abundant chalcogenide photovoltaic materials buffered with CdS: the limiting effect of band alignment. Journal of Physics: Energy, 2(2), 025002.

Hausser, S., Fuchs, G., Hangleiter, A., Streubel, K. andTsang, W. T. (1990). Auger recombination in bulk and quantum well InGaAs. Applied physics letters, 56(10), 913-915.

Kaur, I., Pandya, D. K. and Chopra, K. L. (1980). Growth kinetics and polymorphism of chemically deposited CdS films. Journal of the Electrochemical Society, 127(4), 943.

Mustafa, F. A. (2013). Optical properties of NaI doped polyvinyl alcohol films. Physical Sciences Research International, 1(1), 1-9.

Niane, D., Diagne, O., Ehemba, A. K., Soce, M. M. and Dieng, M. (2018). Generation and Recombination of a CIGSe Solar Cell under the Influence of the Thickness of a Potassium Fluoride (KF) Layer. American Journal of Materials Science and Engineering, 6(2), 26-30.

Patidar, D., Sharma, R., Jain, N., Sharma, T. P. and Saxena, N. S. (2006). Optical properties of CdS sintered film. Bulletin of Materials Science, 29, 21-24.

IJPAS
ijpas@munzur.edu.tr
ISSN: 2149-0910

Research article/Araştırma makalesi
DOI:10.29132/ijpas.1377054

Perna, G., Capozzi, V., Ambrico, M., Augelli, V., Ligonzo, T., Minafra, A., Schiavulli, L. and Pallara, M. (2004). Structural and optical characterization of undoped and indium-doped CdS films grown by pulsed laser deposition. Thin Solid Films, 453, 187-194.

Petrus, R. Y., Ilchuk, H. A., Kashuba, A. I., Semkiv, I. V., Zmiiovska, E. O. and Honchar, F. M. (2020). Optical properties of CdS thin films. Journal of Applied Spectroscopy, 87, 35-40.

Pindolia, G., Shinde, S. M. and Jha, P. K. (2022). Optimization of an inorganic lead free $RbGeI_3$ based perovskite solar cell by SCAPS-1D simulation. Solar Energy, 236, 802-821.

Ravindra, N. M., Ganapathy, P. and Choi, J. (2007). Energy gap–refractive index relations in semiconductors–An overview. Infrared physics & technology, 50(1), 21-29.

Rittner, E. S. and Schulman, J. H. (1943). Studies on the Coprecipitation of Cadmium and Mercuric Sulfides. The Journal of Physical Chemistry, 47(8), 537-543.

Sahay, P. P., Nath, R. K. and Tewari, S. (2007). Optical properties of thermally evaporated CdS thin films. Crystal Research and Technology: Journal of Experimental and Industrial Crystallography, 42(3), 275-280.

Sankapal, B. R., Mane, R. S. and Lokhande, C. D. (2000). Deposition of CdS thin films by the successive ionic layer adsorption and reaction (SILAR) method. Materials research bulletin, 35(2), 177-184.

Seon, J.-B., Lee, S., Kim, J. M. and Jeong, H.-D. (2009). Spin-coated CdS thin films for n-channel thin film transistors. Chemistry of Materials, 21(4), 604-611.

Srivastava, A., Dua, P., Lenka, T. R. and Tripathy, S. K. (2021). Numerical simulations on CZTS/CZTSe based solar cell with ZnSe as an alternative buffer layer using SCAPS-1D. Materials Today: Proceedings, 43, 3735-3739.

Strauss, U., Rühle, W. W. and Köhler, K. (1993). Auger recombination in intrinsic GaAs. Applied Physics Letters, 62(1), 55-57.

Su, B. and Choy, K. L. (2000). Microstructure and properties of the CdS thin films prepared by electrostatic spray assisted vapour deposition (ESAVD) method. Thin Solid Films, 359(2), 160-164.

Tripathi, S., Lohia, P. and Dwivedi, D. K. (2020). Contribution to sustainable and environmentally friendly non-toxic CZTS solar cell with an innovative hybrid buffer layer. Solar Energy, 204, 748-760.

Xu, J., Quan, S., Zou, Z., Guo, P., Lu, Y., Yan, H. and Luo, Y. (2016). Color-tunable photoluminescence from In-doped CdS nanowires. Chemical Physics Letters, 652, 216-219.

Yoon, S. H., Lee, S. S., Seo, K. W. and Shim, I. (2006). Preparation of CdS thin films through MOCVD method, using Cd-S single-source precursors. Bulletin-Korean Chemical Society, 27(12), 2071.

Zelaya, A.O., Alvarado-Gil, J. J., Lozada-Morales, R., Vargas, H. and Ferreira da Silva, A. (1994). Band-gap shift in CdS semiconductor by photoacoustic spectroscopy: Evidence of a cubic to hexagonal lattice transition. Applied Physics Letters, 64(3), 291-293.

Ziabari, A.A. and Ghodsi, F. E. (2012). Growth, characterization and studying of sol–gel derived CdS nanoscrystalline thin films incorporated in polyethyleneglycol: Effects of post-heat treatment. Solar energy materials and solar cells, 105, 249-262.